Article.

The effect of few-layer graphene on the complex of hardness, strength and thermo physical properties of polymer composite materials produced by DLP 3D printing.

Sergey Kidalov* [1], Alexander Voznyakovskii [2], Aleksei Vozniakovskii [1], Sofya Titova [1], Yvgenii Auchynnikau [3]

[1] Ioffe Institute; post@mail.ioffe.ru
[2] Institute of Synthetic Rubber; voznap@mail.ru
[3] Yanka Kupala State University of Grodno; mail@grsu.by
* Correspondence: kidalov@mail.ioffe.ru

Abstract: The results of studying the effect of particles of few-layer graphene (FLG) synthesized by self-propagating high-temperature synthesis (SHS) on the complex of strength and thermo physical properties of polymer composite products obtained by DLP 3D printing are presented. It has been discovered to achieve an increase in thermo physical and strength parameters of polymers modified by FLG compared with samples made on the unmodified base resin. This result was achieved due to low defectiveness, namely the absence of Stone-Wales defects in the structure of FLG due to the homogeneous distribution of FLG over the volume of the polymer in the form of highly dispersed aggregates. It was possible to increase hardness by 120 %, bending strength by 102 %, Charpy impact strength by 205 %, and thermal conductivity at 25 °C by 572 % at concentrations of few-layer graphene of no more than 2 wt. %.

Keywords: photopolymer resin**,** few-layer graphene, FLG, DLP, 3D printing, hardness, bending strength, charpy impact strength, thermal conductivity.

1. Introduction

Currently, there are many 3D printing methods, one of which is the Direct Light Processing (DLP) method. This method is based on the layer-by-layer curing of photopolymer resin and is an evolution of the Stereo lithography (SLA) method. Although the principle of the SLA method itself became known as early as 1986 [1], two years earlier than the fused deposition modeling (FDM) method [2], it was the FDM method that became the most popular 3D printing technique due to much cheaper 3D printers. Now DLP 3D printers have become much cheaper, which has made them available to almost everyone. However, although the DLP method makes it possible to obtain products with high accuracy, low roughness, and relatively quick, products made from photopolymer resins have relatively lower strength characteristics than products obtained by the FDM method.

One of the most promising ways to improve the properties of final products obtained by DLP 3D printing is the use of composite materials [3]. Metal nitrides [4], metal oxides [5], carbon black [6], lignin [7], there mixtures [8] etc., are used as fillers. By combining the properties of the matrix and the filler, researchers obtain final products with higher properties.

To improve the properties of final products, researchers also actively add various carbon nanomaterials, including graphene nanostructures, to the initial photopolymer resins [9]. Interest in graphene nanostructures is due to their record-breaking characteristics. It should be noted that the thermal conductivity of single-layer graphene is about 5000 W/(m*K) [10], and Young's modulus is 1 TPa [11]. These characteristics allow you to

 doi:10.20944/preprints202212.0308.v1

get better results than when using classic fillers. These characteristics will enable you to get better results than when using traditional fillers.

For example, in [12], the authors use no more than 2 wt. % of graphene sheets increased the tensile strength by 2.19 times compared to the original rubber. The authors also noted that the use of graphene nanosheets turned out to be more efficient than using a standard filler - polyaniline fibers, with which only 1.41 times growth was achieved. In [13], the authors increased the flexural modulus and fracture toughness by 14% and 28% from neat resin, respectively, using 0.5 wt. % graphene nanoplates (GNP).

However, the use of graphene nanostructures does not always lead to the expected increase in the properties of the final composites. In [14], the authors showed that the introduction of 0.5 and 1 wt. % GNP only resulted in a deterioration in Young's modulus, tensile strength and other strength characteristics compared to pure rubber.

The reason for such different results in different groups of researchers can be explained by using graphene nanostructures with varying degrees of defectiveness. Defects significantly affect the final properties of the graphene nanostructures themselves [15] and, accordingly, the properties of composites modified with graphene nanostructures.

In our previous work [16], we showed the possibility of synthesizing FLG under self-propagating high-temperature synthesis (SHS) conditions from cyclic biopolymers. An important advantage of FLG synthesized by this method is the absence of Stone–Wales defects [17], which is almost inevitable in synthesis by other methods. We found that FLG nanostructures synthesized by the SHS method could significantly improve nitrile butadiene rubber's complex strength and thermo physical properties [18].

In this paper, we consider the effect of FLG synthesized by the SHS process on a complex of strength and thermo physical properties of products from photopolymer resins obtained by DLP 3D printing.

2. Materials and Methods

2.1. Raw materials

A commercial photopolymer resin of the Anycubic brand (405 nm, clear, China) was taken as the starting material for obtaining products using the DLP 3D printing method.

The procedure for obtaining FLG is described in detail in [16, 19]. The particles of FLG synthesized by the SHS method were taken as a modifying additive. The particles have an average lateral size of up to 20 μm and consist of no more than 5 graphene layers. There are no Stone-Wales defects in this material, which was shown in [17].

2.2. SEM and TEM studies

SEM and TEM studies of the morphology and structure of FLG nanoparticles were carried out using the TESCAN Mira-3M (Brno, Czech Republic) and FEI Tecnai G2 30 S-TWIN (50 kV) microscope.

2.3. Measurement of dispersion of FLG particles

Particle dispersity was measured on a Zetasizer nano ZS instrument.

2.4. Obtaining products from photopolymer resins with the addition of FLG.

The scheme for obtaining samples from photopolymer resins with the addition of FLG is shown in Figure 1.

 doi:10.20944/preprints202212.0308.v1

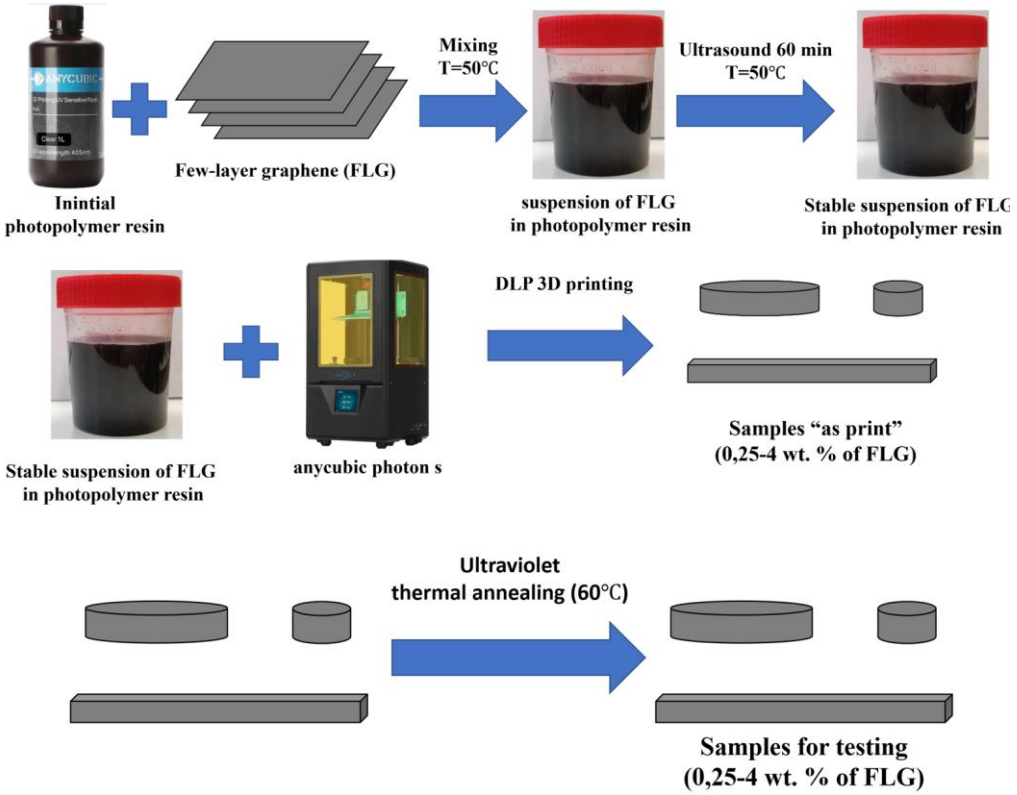

Figure 1. Scheme for obtaining samples from photopolymer resins with the addition of FLG.

In the original photopolymer resin (Anycubic brands, 405 nm, clear) heated to 50 °C in uniform portions (0.1 of the entire sample), FLG powder was sequentially added with constant stirring using an overhead stirrer (500 rpm).

The concentration of the additive ranged from 0.25 to 4 wt. %, which corresponded to 0.475 to 7.6 vol. %.

Then, the resulting suspension was kept in the ultrasound field for 1 hour (ultrasonic tub, 22 kHz) while maintaining the temperature at 50 °C until a stable suspension was obtained. The cooled photopolymer resin with FLG was placed in the "Anycubic Photon S" DLP 3D printer, and samples of the required sizes were made. Printing parameters: illumination layer thickness 50 microns, exposure time 6 seconds. Figure 2 shows typical synthesized samples.

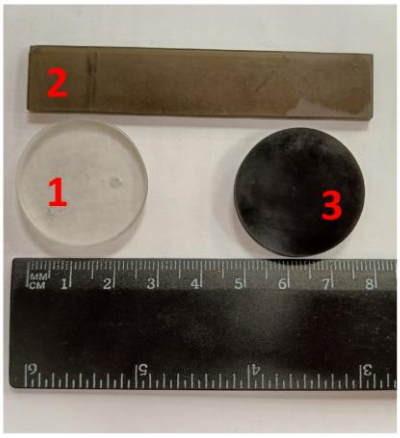

Figure 2. Samples of products obtained by DLP 3D printing. 1 - initial resin, 2 – 0,25 wt. % FLG, 3 - 2 wt. % FLG.

 doi:10.20944/preprints202212.0308.v1

Then the obtained samples were sequentially subjected to UV treatment for 1-2 hours and thermal annealing for 1-2 hours.

2.5. Viscosity measurement

The viscosity of stable suspensions of FLG in photopolymer resins was measured on a rotational viscometer NDJ-9S (China) using a thermostat (WEST TUNE, China), with temperature maintenance accuracy ±0.1 °C.

2.6. Hardness test

The measurement of hardness by the Brinell method (ISO 506-81) was carried out on a hardness tester Metrotest ITB-3000 AM.

The dimensions of the prints were determined using an image analysis system. Based on this data, the hardness of the material was calculated.

Samples in the form of discs 30 mm in diameter and 5 mm thick were prepared for hardness testing.

2.7. Measurement of bending strength

The bending strength was measured on a PM-MG4 hydraulic press in accordance with ISO 178:2010. For bending strength tests, samples were made in the form of beams with a length of 80 mm, a width of 15 mm, a height of 3 mm.

2.8. Measurement of Charpy impact strength

Obtaining data on the impact strength of composites (impact in the rib) was obtained on a Koper pendulum KMM-50 (RF) by ISO 179-1:2010. Samples were prepared in the form of beams (without notch) with a length of 80 mm, a width of 10 mm, and a height of 4 mm, the distance between the supports was 60 mm.

2.9. Measurement of thermal conductivity and heat capacity

Thermal conductivity and heat capacity were measured using a DXF-200 flash method (using a xenon lamp) at 25 °C. The samples were cylinders 10 mm in diameter and 1 mm thick. One side of the sample was covered with a thin layer of graphite paint (for the complete absorption of the flash energy) to improve the experiment's accuracy. The heat capacity measurement accuracy was ±7 %, and the thermal conductivity measurement accuracy was ±5 %.

3. Results and discussion

Dynamic viscosity is an important parameter that affects the usability of photopolymer resin. The results of measuring the dynamic viscosity of the resulting FLG suspensions in the photopolymer resin are shown in Figure 3.

Preprints (www.preprints.org) | NOT PEER-REVIEWED | Posted: 16 December 2022 doi:10.20944/preprints202212.0308.v1

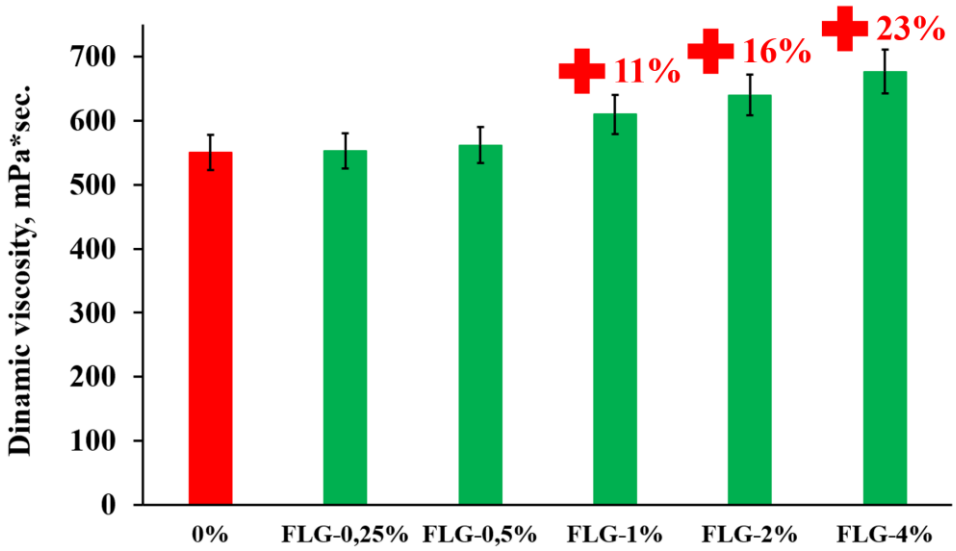

Figure 3. Dependence of the dynamic viscosity of stable suspensions of photopolymer resins at 25 °C depending on the concentration of FLG.

As can be seen from Figure 3, the introduction of FLG at a concentration of more than 1 wt. % leads to a slight increase in dynamic viscosity. The introduction of graphene nanostructures often leads to a greater increase in dynamic viscosity at such concentrations, as was shown in [20, 21]. Therefore, a study was made of the dispersion of FLG particles in a photopolymer resin before and after ultrasonic treatment at 50 °C. The measurement results are shown in Figure 4.

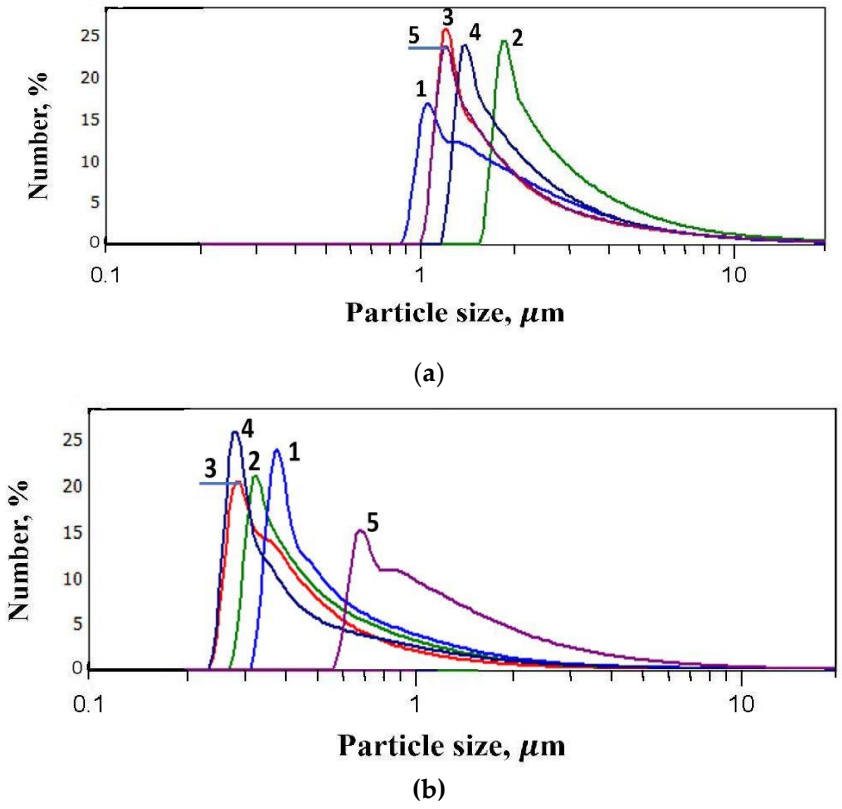

Figure 4. Results of measurements of the dispersion of FLG particles in a photopolymer resin. (a) - without ultrasonic treatment, 1 - 0.25 wt. %, 2 - 0.5 wt. %, 3 – 1 wt. %, 4 – 2 wt. %, 5 – 4 wt. %; (b) - ultrasonic treatment at 50 °C, 1 - 0.25 wt. %, 2 - 0.5 wt. %, 3 – 1 wt. %, 4 – 2 wt. %, 5 – 4 wt. %.

 doi:10.20944/preprints202212.0308.v1

As can be seen from Figure 4, the dispersion of FLG particles after ultrasonic treatment changes significantly from 1.2–1.4 μm to 250–300 nm. It should be noted that a similar measurement of dispersion occurs at other concentrations (0.25; 0.5; 2; 4 wt. %).

Such a significant increase in dispersion, in combination with a substantial decrease in the viscosity of the photopolymer resin due to heating, makes it possible to evenly distribute FLG particles throughout the volume, which leads to a relatively low increase in dynamic viscosity.

Post-processing (ultraviolet irradiation, thermal annealing) of 3D printed samples can significantly improve the final complex of product properties. Therefore, we investigated the effect of a combination of post-processing techniques (UV treatment and annealing at 70 °C) and their duration on the hardness of the final products. The results are presented in Table 1.

Table 1. Dependence of Brinell hardness on post-processing techniques and their duration.

Post-processing technique	Brinell hardness	Change, %
No processing	5,6±0,3	0
1 hour UV	7,4±0,4	32
1 hour annealing	6,1±0,3	9
1 hour UV+1 hour annealing	10,6±0,5	89
1 hour UV + 2 hours annealing	8,8±0,4	57
2 hours UV + 1 hour annealing	10,2±0,5	82
2 hours UV + 2 hours annealing	8,2±0,4	46

As can be seen from Table 1, 1-hour UV treatment followed by 1 hour annealing gave the best results, so this post-processing was used for all further samples.

Figure 5 shows the results of studying the structure of the obtained products by the SEM method.

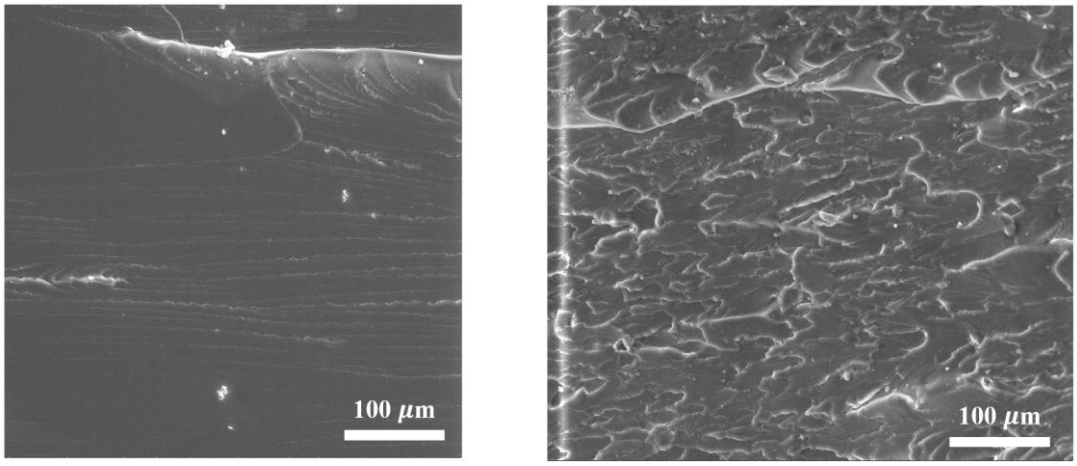

(**a**) (**b**)

 doi:10.20944/preprints202212.0308.v1

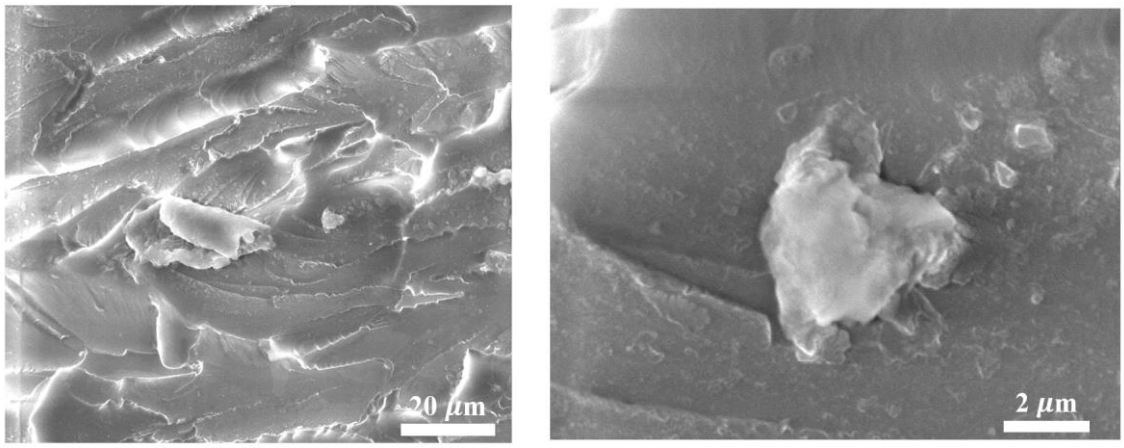

(c) **(d)**

Figure 5. SEM images of **(a)** cleavage sample from the original resin (linear scale 100 μm); **(b)** modified 1 wt. % FLG (linear scale 100 μm); **(c)** modified 1 wt. % FLG (linear scale 20 μm); **(d)** modified 1 wt. % FLG (linear scale 2 μm).

As seen from Figure 5(b-d), FLG particles in the polymer composite are distributed in the form of aggregates of various fineness, consistent with the result of measuring fineness by the DLS method.

Figure 6 shows the results of measuring the Brinell hardness of the synthesized samples.

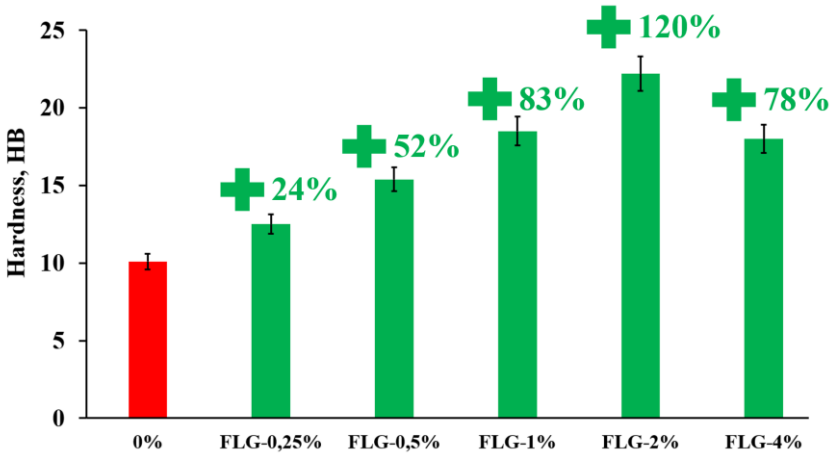

Figure 6. Brinell hardness of samples depends on the concentration of FLG.

As seen in Figure 6, the introduction of FLG makes it possible to increase the Brinell hardness up to 120 % compared to a pure sample at an FLG concentration of 2 wt. %. A further increase in the concentration of FLG does not lead to a further increase in hardness.

Figures 7 and 8 show the results of measuring the flexural strength of the obtained composites.

Preprints (www.preprints.org) | NOT PEER-REVIEWED | Posted: 16 December 2022 doi:10.20944/preprints202212.0308.v1

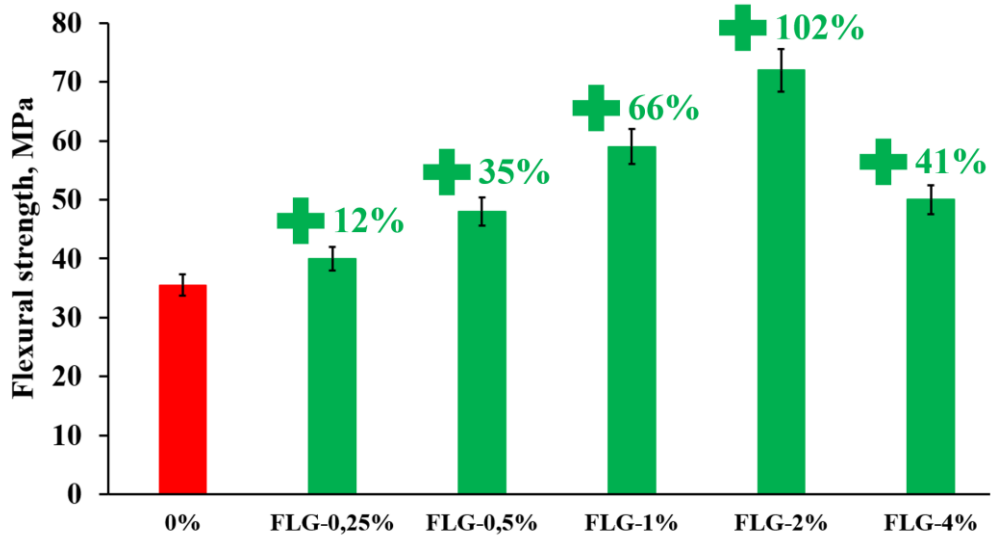

Figure 7. Flexural strength of samples depending on the concentration of FLG.

As seen in Figure 7, the introduction of FLG makes it possible to increase the flexural strength up to 102 % compared to a pure sample at an FLG concentration of 2 wt. %. A further increase in the concentration of FLG does not lead to a further increase in the flexural strength.

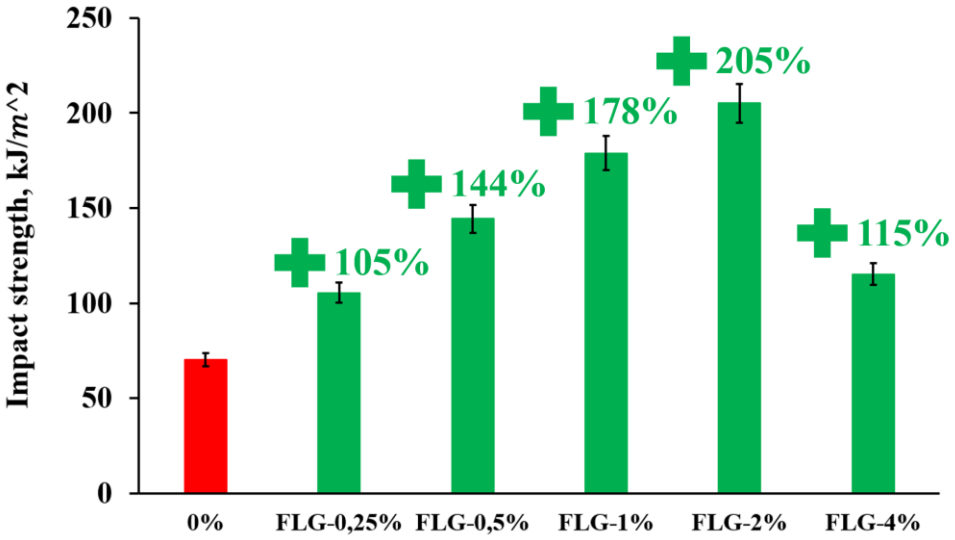

Figure 8. Charpy impact strength of the samples depending on the concentration of FLG.

As seen in Figure 8, the introduction of FLG makes it possible to increase the Charpy impact strength up to 205 % compared to a pure sample at an FLG concentration of 2 wt. %. A further increase in the concentration of FLG does not lead to a further increase.

The data on the effect of FLG on the complex strength properties of final products (hardness, bending strength, impact strength) shows that FLG can significantly improve the properties of final composites. An increase in the properties of products upon the addition of graphene nanostructures to polymer matrices has been repeatedly observed in other works, for example, [22, 23]. In classical models, the authors assume that particles of graphene nanostructures are reinforcing agents that distribute the load over the entire matrix and prevent crack propagations [24].

Preprints (www.preprints.org) | NOT PEER-REVIEWED | Posted: 16 December 2022 doi:10.20944/preprints202212.0308.v1

The efficiency of using graphene nanostructures in the creation of composites critically depends on the uniformity of their distribution, fineness, and the presence and concentration of various structural defects.

Based on this, and considering the DLS data (Figure 4), it can be assumed that the results obtained are due to the uniform distribution of FLG particles that do not have Stone-Wales defects in their structure. That can be considered as highly dispersed graphene aggregates in polymers.

Figure 9 shows the results of measuring the synthesized products' thermal conductivity and heat capacity.

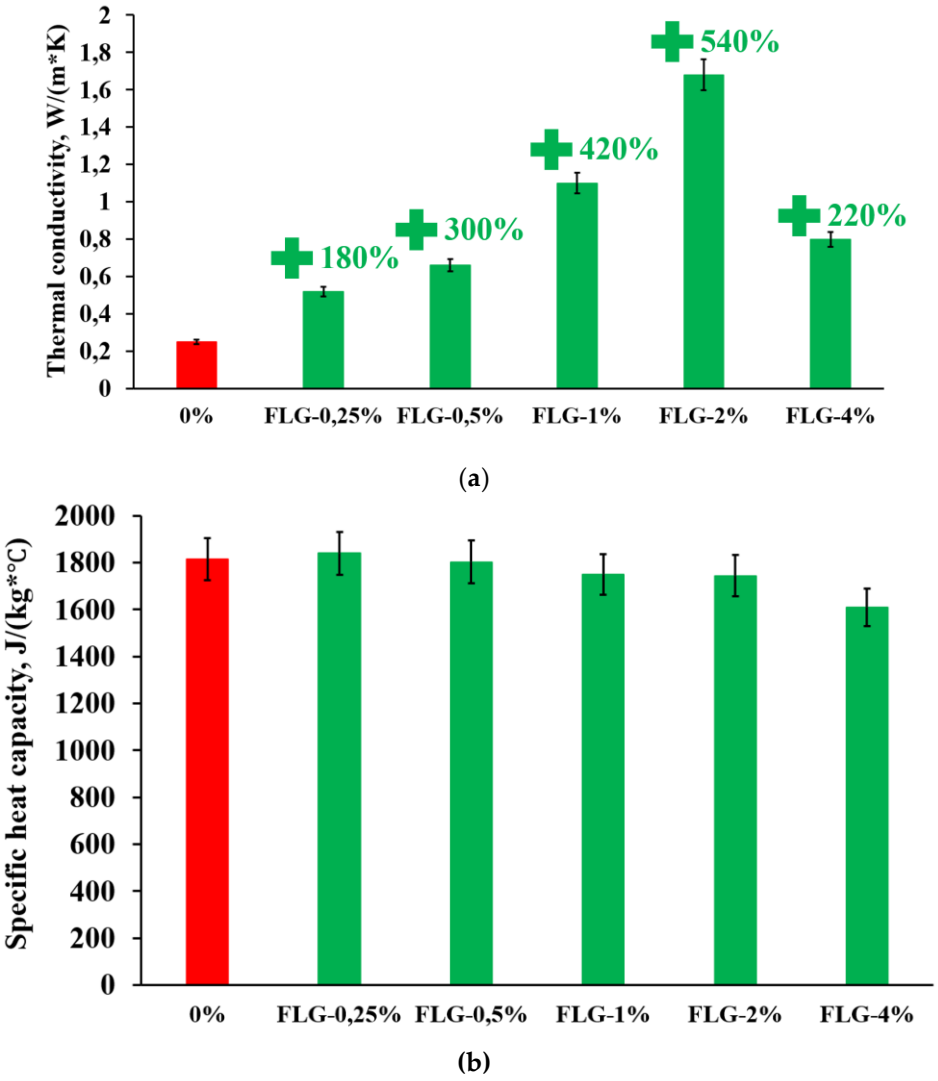

Figure 9. Dependence of thermal conductivity **(a)** and specific heat capacity **(b)** of synthesized samples on FLG concentration at 25 °C.

As seen in Figure 9, the introduction of FLG makes it possible to increase the thermal conductivity up to 540 % compared to a pure sample at an FLG concentration of 2 wt. %.

However, the synthesized samples' specific heat capacity remains unchanged (within the method error). This is because the heat capacity of graphene nanostructures is estimated at 700 J/(kg*°C) [25], which leads to a gradual decrease in the heat capacity of the composite with an increase in the proportion of FLG.

Preprints (www.preprints.org) | NOT PEER-REVIEWED | Posted: 16 December 2022 doi:10.20944/preprints202212.0308.v1

Some calculations were carried out using various thermal conductivity models to determine the mechanism of change in thermal conductivity in the obtained composites.

To compare the obtained experimental data with various models of thermal conductivity of composite materials, the volume fractions of FLG in the synthesized composite were calculated from the measured density of composites and the mass fraction of FLG.

For the simplest assessment of the thermal conductivity of composite material, a geometric model can be used.

The volume fractions of FLG in the synthesized composite were calculated from the measured density of composites and the mass fraction of FLG to compare the obtained experimental data with various models of thermal conductivity of composite materials.

A geometric model can be used for the simplest assessment of the thermal conductivity of composite material [26].

$$\lambda_c = \lambda_m^{v_m} * \lambda_f^{v_f} \quad (1)$$

Where λ_c — thermal conductivity of composite material (W/(m K)), λ_m =0,25 — thermal conductivity of the matrix (W/(m K)), λ_f — thermal conductivity of the filler (W/(m K)), υ_m — volume fraction of the matrix, %, υ_f — volume fraction of the filler, %.

To calculate the theoretical values of the thermal conductivity of polymer composites, researchers often use the Maxwell model [27]:

$$\lambda_c=\lambda_m*(\lambda_f+2*\lambda_m-2*\upsilon_f*(\lambda_m-\lambda_f))/(\lambda_f+2*\lambda_m+\upsilon_f*(\lambda_m-\lambda_f)) \quad (2)$$

However, the Maxwell model assumes that the filler particles are spherical. Therefore, to account for the thin sheets shape of the filler FLG particles, we use Maxwell–Burger–Eiken (MBE) model [28]:

$$\lambda_c=\lambda_m*((1-(1-\lambda_f/\lambda_m)*L*\upsilon_f)/(1+(L-1)*\upsilon_m) \quad (3)$$

Where $L = (\lambda_m+2*\lambda_f)/(3*\lambda_m)$ is the coefficient taking into account, the thin sheets shape of the FLG filler particles.

It should be noted that although the thermal conductivity of graphene is estimated at up to 5000 W/(m*K), aggregates of graphene particles have orders of magnitude lower thermal conductivity, which is due to energy losses at particle boundaries. This fact is one of the reasons for the discrepancy between theoretical calculations and experimental data [29]. Using experimental data on the thermal conductivity of the composite with 1 wt. % FLG and the models described above, the thermal conductivity of aggregates of FLG particles was evaluated (Table 2).

Table 2 The results of calculations of the thermal conductivity of the composite with 1 wt. % FLG for various models depending on the thermal conductivity of FLG aggregates.

υ_m, %	υ_f, %	λ_m,	λ_f,	λ_c, Geometric model	λ_c, Maxwell model	λ_c, MBE model	λ_c, Experimental value

 doi:10.20944/preprints202212.0308.v1

%	%			W/(m*K)			
0,981	0,019	0,25	0,5	0,265	0,254	0,27	
0,981	0,019	0,25	5	0,265	0,263	0,41	
0,981	0,019	0,25	50	0,265	0,264	0,86	1,1±0,05
0,981	0,019	0,25	500	0,265	0,265	1,86	
0,981	0,019	0,25	5000	0,265	0,265	10,12	
0,981	0,019	0,25	0,5	0,265	0,254	0,27	

As seen from Table 2, the change in the thermal conductivity of the filler for the geometric model and the Maxwell model practically does not change the calculated result. In the case of the MBE model, the thermal conductivity value drastically changes the final calculated value of the thermal conductivity of the composite. Having carried out an additional selection of values for the MBE model, it was found that the thermal conductivity of FLG particle aggregates can be estimated at 40 W/(m*K), which was taken for further calculations. The calculation results are shown in Figure 10.

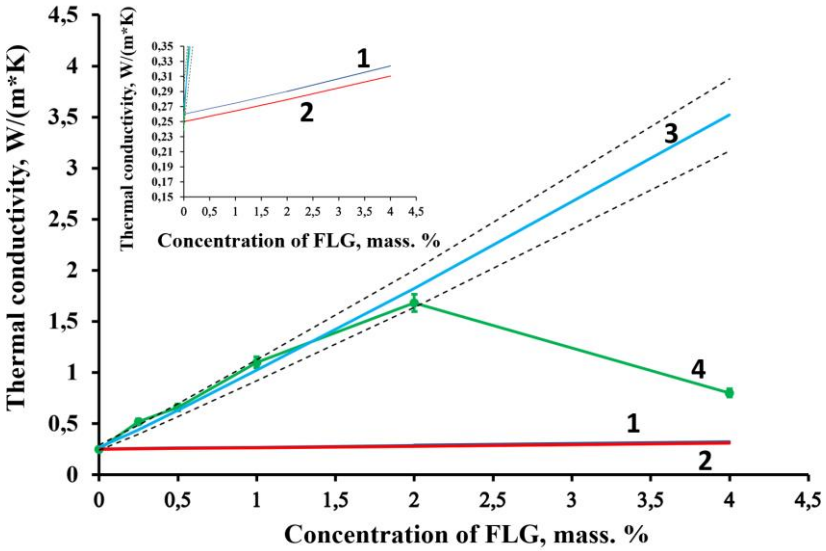

Figure 10. Comparison of experimental data with the results of calculations by models. 1 - geometric model; 2 – Maxwell model; 3 - MBE model; 4 - experimental data. The dotted line shows a 10 % deviation from the MBE model.

As can be seen from Figure 10, in contrast to the geometric model and the Maxwell model, which give greatly underestimated values compared to the experimental data, the MBE model gives an acceptable agreement with the experimental data up to 2 wt. % of FLG. These results are because, in the geometric model and the Maxwell model, it is assumed that the filler particles have a spherical shape and do not interact with each other. In contrast, the MBE model is where the lamellar shape of the filler particles is taken into account.

The dropout point at a concentration of FLG in 4 wt. % is due to an increase in the size of FLG aggregates, which is confirmed by the DLS data (Figure 4), and, accordingly, a decrease in their thermal conductivity. The solution of the inverse problem for experimental data on thermal conductivity at 4 wt. % showed that the thermal conductivity of aggregates could be estimated at about 5-6 W/(m*K).

4. Conclusions

FLG particles synthesized under the conditions of the SHS process have shown themselves to be effective fillers capable of significantly increasing the complexity of strength and thermo physical properties of polymer composite products obtained by the DLP 3D printing method. This effect was achieved due to a combination of low defectiveness of FLG particles, as well as a highly efficient dispersion technique, which made it possible to distribute finely dispersed FLG particles in polymer evenly.

As a result, it was possible to increase hardness and flexural strength by 2 times, impact strength by 3 times and thermal conductivity at 25 °C by 6 times at concentrations of FLG 2 wt. %.

In further work, it is necessary to investigate the influence of 3D printing parameters such as layer thickness and layer exposure time on the final properties of polymer composite products.

Author Contributions: Conceptualization, Alexander Voznyakovskii and Aleksei Vozniakovskii; Formal analysis, Sofya Titova and Yvgenii Auchynnikau; Funding acquisition, Sergey Kidalov; Investigation, Aleksei Vozniakovskii and Sofya Titova; Methodology, Aleksei Vozniakovskii; Resources, Yvgenii Auchynnikau; Supervision, Sergey Kidalov; Visualization, Sergey Kidalov; Writing – original draft, Sergey Kidalov and Aleksei Vozniakovskii; Writing – review & editing, Sergey Kidalov.

Funding: "This research was funded by the frame of the Government Topical Program for Ioffe Institute (project 0040-2014-0013 "Physical-chemical basics of technology for new functional materials based on carbon nanostructures")

Conflicts of Interest: The authors declare no conflict of interest.

References

1. Hull, C.W. Apparatus for Production of Three-Dimensional Objects by Stereolithography. U.S. Patent 4575330A, 11 March 1986.

2. Crump, S.S. Rapid prototyping using FDM. *Mod. Cast.* **1992**, *82*, 36-38.

3. Blanco, I. The Use of Composite Materials in 3D Printing. *J. Compos. Sci.* **2020**, *4*, 42. https://doi.org/10.3390/jcs4020042

4. Lee, S., Kim, Y., Park, D., Kim, J. The thermal properties of a UV curable acrylate composite prepared by digital light processing 3D printing. *Compos. Commun.* **2021**, *26*, 100796. DOI: 10.1016/j.coco.2021.100796

5. Chaudhary, R., Fabbri, P., Leoni, E., Mazzanti, F., Akbari, R., Antonini, C. Additive manufacturing by digital light processing: a review. *Prog. Addit. Manuf.* **2022**, 1-21. DOI: 10.1007/s40964-022-00336-0

6. Zheng, Y., Huang, X., Chen, J., Wu, K., Wang, J., Zhang, X. A review of conductive carbon materials for 3D printing: Materials, technologies, properties, and applications. *Materials* **2021**, *14*, 3911. DOI: 10.3390/ma14143911

7. Arias-Ferreiro, G., Lasagabáster-Latorre, A., Ares-Pernas, A., Ligero, P., García-Garabal, S. M., Dopico-García, M. S., Abad, M. J. (2022). Lignin as a High-Value Bioaditive in 3D-DLP Printable Acrylic Resins and Polyaniline Conductive Composite. *Polymers* **2022**, *14(19)*, 4164. DOI: 10.3390/polym14194164

8. Ibrahim, F., Mohan, D., Sajab, M. S., Bakarudin, S. B., Kaco, H. Evaluation of the compatibility of organosolv lignin-graphene nanoplatelets with photo-curable polyurethane in stereolithography 3D printing. *Polymers* **2019**, *11(10)*, 1544. DOI: 10.3390/polym11101544

9. Ponnamma, D., Yin, Y., Salim, N., Parameswaranpillai, J., Thomas, S., Hameed, N. (2021). Recent progress and multifunctional applications of 3D printed graphene nanocomposites. *Composites, Part B* **2021**, *204*, 108493. DOI: 10.1016/j.compositesb.2020.108493

10. Balandin, A. A., Ghosh, S., Bao, W., Calizo, I., Teweldebrhan, D., Miao, F., Lau, C. N. Superior thermal conductivity of single-layer graphene. *Nano Lett.* **2008**, *8(3)*, 902-907. DOI: 10.1021/nl0731872

11. Lee, C., Wei, X., Kysar, J. W., Hone, J. Measurement of the elastic properties and intrinsic strength of monolayer graphene. *Science* **2008**, *321(5887)*, 385-388. DOI: 10.1126/science.1157996

12. Joo, H.; Cho, S. Comparative Studies on Polyurethane Composites Filled with Polyaniline and Graphene for DLP-Type 3D Printing. *Polymers* **2020**, *12*, 67. https://doi.org/10.3390/polym12010067

13. Feng Z, Li Y, Xin C, Tang D, Xiong W, Zhang H. Fabrication of Graphene-Reinforced Nanocomposites with Improved Fracture Toughness in Net Shape for Complex 3D Structures via Digital Light Processing. *C.* **2019**, *5(2)*, 25. https://doi.org/10.3390/c5020025

14. Hanon, M. M., Ghaly, A., Zsidai, L., Szakál, Z., Szabó, I., & Kátai, L. (2021). Investigations of the Mechanical Properties of DLP 3D Printed Graphene/Resin Composites. *Acta Polytech. Hung.* **2021**, *18(8)*, 143-161. DOI: 10.12700/APH.18.8.2021.8.8

15. Xu, T., Sun, L. Structural defects in graphene. In *Defects in Advanced Electronic Materials and Novel Low Dimensional Structures.* Stehr, J., Buyanova, I., Chen, W. Woodhead Publishing. Sawston, Cambridge, UK, **2018**, 137-160. DOI: 10.1016/B978-0-08-102053-1.00005-3

16. Voznyakovskii, A., Vozniakovskii, A., Kidalov, S. New Way of Synthesis of Few-Layer Graphene Nanosheets by the Self Propagating High-Temperature Synthesis Method from Biopolymers. *Nanomaterials* **2022**, *12(4)*, 657. DOI: 10.3390/nano12040657

17. Voznyakovskii, A., Neverovskaya, A., Vozniakovskii, A., Kidalov, S. A Quantitative Chemical Method for Determining the Surface Concentration of Stone–Wales Defects for 1D and 2D Carbon Nanomaterials. *Nanomaterials* **2022**, *12(5)*, 883. DOI: 10.3390/nano12050883

18. Vozniakovskii, A.A., Voznyakovskii, A.P., Kidalov, S.V., Otvalko, J, Neverovskaia, A. Yu. Characteristics and mechanical properties of composites based on nitrile butadiene rubber using graphene nanoplatelets, *J. Compos. Mater.* **2020**, *54(23)*, 3351-3364. DOI: 10.1177/0021998320914366.

19. Vozniakovskii A.A., Voznyakovskii A.P., Kidalov S.V., Osipov V. Yu, Structure and Paramagnetic Properties of Graphene Nanoplatelets Prepared from Biopolymers Using Self-Propagating High-Temperature Synthesis, *J. Struct. Chem.* **2020**, *65(5)*, 869-878. DOI: 10.1134/S0022476620050200

20. Parente, J. M., Simões, R., Reis, P. N. B. Effect of graphene nanoparticles on suspension viscosity and mechanical properties of epoxy-based nanocomposites. *Procedia Struct. Integr.* **2022**, *37*, 820-825. DOI: 10.1016/j.prostr.2022.02.014

21. Zhao, R., Jing, F., Li, C., Wang, R., Xi, Z., Cai, J.,Wang, Q., Xie, H. Viscosity-curing time behavior, viscoelastic properties, and phase separation of graphene oxide/epoxy asphalt composites. *Polym. Compos.* **2022**, *43(8)*, 5454-5464. DOI: 10.1002/pc.26848

22. Erkliğ, A., Doğan, N. F., Bulut, M. Charpy impact response of glass fiber reinforced composite with nano graphene enhanced epoxy. *Period. Eng. Nat. Sci.* **2017**, *5(3)*; DOI: 10.21533/pen.v5i3.121

23. Manapat, J. Z., Mangadlao, J. D., Tiu, B. D. B., Tritchler, G. C., Advincula, R. C. High-strength stereolithographic 3D printed nanocomposites: graphene oxide metastability. *ACS Appl. Mater. Interfaces* **2017**, *9(11)*, 10085-10093. DOI: 10.1021/acsami.6b16174

24. Papageorgiou, D. G., Li, Z., Liu, M., Kinloch, I. A., Young, R. J. Mechanisms of mechanical reinforcement by graphene and carbon nanotubes in polymer nanocomposites. *Nanoscale* **2020**, *12(4)*, 2228-2267. DOI: 10.1039/C9NR06952F

25. Li, Q. Y., Xia, K., Zhang, J., Zhang, Y., Li, Q., Takahashi, K., Zhang, X. Measurement of specific heat and thermal conductivity of supported and suspended graphene by a comprehensive Raman optothermal method. *Nanoscale* **2017**, *9(30)*, 10784-10793. DOI: 10.1039/C7NR01695F

26. Progelnof, R.C., Throne, J.L. Reutsch, R.R. Methods of predicting the thermal conductivity of composite systems: a review. *Polym Eng Sci.* **1976**; *16*, 615–625. DOI: 10.1002/pen.760160905

 doi:10.20944/preprints202212.0308.v1

27. Zhai, S., Zhang, P., Xian, Y., Zeng, J., Shi, B. Effective thermal conductivity of polymer composites: Theoretical models and simulation models. *Int. J. Heat Mass Transfer.* **2018**, *117*, 358-374. DOI: 10.1016/j.ijheatmasstransfer.2017.09.067

28. Baranovskii, V. M., Temnikova, S. V., Cherenkov, A. V., Zeleneva, T. P., Zelenev, Y. V. Predicting the thermophysical properties of polymer composites using model representations. *Int Polym Sci Technol.* **2004**; *31*, 5–12. DOI: 10.1177/0307174X0403101102.

29. Colonna, S., Battegazzore, D., Eleuteri, M., Arrigo, R., Fina, A. Properties of Graphene-Related Materials Controlling the Thermal Conductivity of Their Polymer Nanocomposites. *Nanomaterials* **2020**, *10(11)*, 2167. DOI: 10.3390/nano10112167